

# Redundancy of Mammalian Proteasome $\beta$ Subunit Function during Endoplasmic Reticulum Associated Degradation<sup>†</sup>

Jon Oberdorf, Eric J. Carlson, and William R. Skach\*

Molecular Medicine Division, Department of Cell and Developmental Biology, and Department of Physiology and Pharmacology, Oregon Health Sciences University, Portland, Oregon 97201

Received June 25, 2001; Revised Manuscript Received August 27, 2001

**ABSTRACT:** Misfolded proteins in the endoplasmic reticulum (ER) are degraded by N-terminal threonine proteases within the 26S proteasome. Each protease is formed by an activated  $\beta$  subunit,  $\beta_5/X$ ,  $\beta_1/Y$ , or  $\beta_2/Z$ , that exhibits chymotrypsin-like, peptidylglutamyl-peptide hydrolyzing, or trypsin-like activity, respectively. Little is known about the relative contribution of specific  $\beta$  subunits in the degradation of endogenous protein substrates. Using active site proteasome inhibitors and a reconstituted degradation system, we now show that all three active  $\beta$  subunits can independently contribute to ER-associated degradation of the cystic fibrosis transmembrane conductance regulator (CFTR). Complete inactivation (>99.5%) of the  $\beta_5/X$  subunit decreased the rate of ATP-dependent conversion of CFTR to trichloroacetic acid soluble fragments by only 40%. Similarly, proteasomes containing only active  $\beta_1/Y$  or  $\beta_2/Z$  subunits degraded CFTR at ~50% of the rate observed for fully functional proteasomes. Simultaneous inhibition (>93%) of all three  $\beta$  subunits blocked CFTR degradation by ~90%, and inhibition of both protease and ATPase activities was required to completely prevent generation of small peptide fragments. Our results demonstrate both a conserved hierarchy (ChT-L > PGPH  $\geq$  T-L) as well as a redundancy of  $\beta$  subunit function and provide insight into the mechanism by which active site proteasome inhibitors influence degradation of endogenous protein substrates at the ER membrane.

The ubiquitin proteasome pathway plays a major role in the quality control and regulated degradation of misfolded, damaged, and unassembled proteins in the endoplasmic reticulum (ER)<sup>1</sup> (1, 2). This process involves substrate ubiquitination, recognition by the 19S regulatory proteasome subunit, and unfolding and delivery of the polypeptide into the core of the 20S proteasome, a toroidal cylinder comprised of four stacked heptameric rings [reviewed in (3); Voges, 1999, #1000]. In eukaryotes, the two inner rings of the 20S proteasome each contain seven  $\beta$  subunits, three of which are proteolytically activated to generate N-terminal threonine proteases (4–7). Active  $\beta$  subunits,  $\beta_5$ ,  $\beta_1$ , and  $\beta_2$ , have been functionally characterized to preferentially cleave substrates after hydrophobic, acidic, and basic residues, respectively, and are thus primarily responsible for the chymotrypsin-like (ChT-L), peptidylglutamyl-peptide hydrolyzing (PGPH), and trypsin-like (T-L) activities observed for eukaryotic proteasomes (8, 9).

Recent studies have suggested that while all active proteasome  $\beta$  subunits participate in substrate degradation, they do not necessarily contribute equally (5, 9, 10). In yeast, genetic inactivation of  $\beta_2/Pup1$  and  $\beta_1/Pre3$  subunits results in mild or no phenotypic changes (11, 12), whereas inactivation of the  $\beta_5/Pre2/Doa3$  subunit effectively inhibits cell growth, protection from stress, and in vivo degradation of ubiquitinated proteins (4). Determining the rank order of importance of these specific activities has been complicated by secondary effects on proteasome maturation efficiency, particularly for active site mutants in  $\beta_2/Pup1$  and  $\beta_5/Pre2/Doa3$  subunits (9). In vitro studies, however, showed that purified yeast 20S proteasomes lacking functional  $\beta_5$  subunits were able to degrade peptides and the protein substrate enolase into fragments similar, but not identical, to those generated by wild-type proteasomes (8, 13). Thus, yeast  $\beta_2$  and  $\beta_1$  subunits can at least partially compensate for loss of  $\beta_5$  activity. Although this also appears to be the case for mammalian proteasomes (8, 14), less is known about the physiologic role of individual mammalian  $\beta$  subunits, in part because genetic mutants are unavailable and because of the difficulty in directly monitoring substrate degradation (i.e., formation of trichloroacetic acid (TCA)-soluble peptide fragments) under in vivo conditions.

Proteasome-mediated ER-associated degradation (ERAD) poses a particular challenge because substrate and degradation machinery are located in different cellular compartments. Luminal domains and transmembrane (TM) segments of integral membrane proteins not only must be unfolded, but must also undergo retrograde translocation and/or extraction from the lipid bilayer in order to reach proteolytic sites within

<sup>†</sup> This work was supported in part by the Cystic Fibrosis Foundation and National Institutes of Health Grants GM53457 and DK51818 (W.R.S.) and T32 DK07674 (J.O.). W.R.S. is an established investigator of the American Heart Association.

\* Correspondence should be addressed to this author at the Molecular Medicine Division, Oregon Health Sciences University, 3181 SW Sam Jackson Park Rd., Portland, OR 97201. Phone: 503-494-7322. Fax: 503-494-1933. E-mail: skachw@ohsu.edu.

<sup>1</sup> Abbreviations:  $\beta$ -lactone, clasto-lactacystin  $\beta$ -lactone; ChT-L, chymotrypsin-like; CFTR, cystic fibrosis transmembrane conductance regulator; PGPH, peptidylglutamyl-peptide hydrolyzing; DTT, dithiothreitol; ER, endoplasmic reticulum; ERAD, ER-associated degradation; LLE, Cbz-Leu-Leu-Glu 7-amido-4-methylcoumarin; LLVY, N-succinyl-Leu-Leu-Val-Tyr 7-amido-4-methylcoumarin; LRR, N-tert-Boc-Leu-Arg-Arg 7-amido-4-methylcoumarin; MG132, Cbz-Leu-Leu-Leu-al; RRL, rabbit reticulocyte lysate; T-L, trypsin-like; TM, transmembrane.

the 20S particle (1, 15). One way that the cell has overcome this problem is to couple membrane extraction and proteolytic cleavage events (15–17). For certain proteins, however, and under conditions of proteasome inhibition, retrograde translocation may precede and be independent of degradation (18–22).

A well-established ERAD substrate is the cystic fibrosis transmembrane conductance regulator (CFTR), a polytopic protein with 12 transmembrane segments, a cytosolic regulatory domain, and 2 large cytosolic nucleotide binding domains (23). Approximately 70–80% of wild-type and nearly 100% of certain mutant CFTR molecules are degraded in the ER by the ubiquitin–proteasome pathway (24, 25). It is generally thought that degradation of both wild-type and mutant CFTR occurs because the newly synthesized protein fails to fold properly (2).

Until recently it has been difficult to examine the relative contribution of  $\beta$  subunits to the degradation of endogenous ER substrates under conditions that approximate the intracellular environment (22). To address this issue, we developed an in vitro, rabbit reticulocyte lysate (RRL)-based system that reconstitutes the key features of CFTR biogenesis and proteasome-mediated degradation (16). In RRL, newly synthesized, core-glycosylated, and membrane-integrated CFTR is rapidly and efficiently ubiquitinated and degraded. Moreover, both the extent and the rate of degradation can be determined by directly monitoring the conversion of CFTR into TCA-soluble peptide fragments. Degradation is ATP-dependent and is insensitive to a wide range of nonproteasome protease inhibitors, but sensitive to hemin [an inhibitor of proteasome ATPase activity (26)] and the peptide aldehyde MG132 (27). In contrast, CFTR degradation was only weakly sensitive to other proteasome inhibitors such as acetyl-Leu-Leu-Nle (ALLN), lactacystin, and its active metabolite *clasto*-lactacystin  $\beta$ -lactone (16). These findings suggest either that certain proteasome inhibitors might be inactive in the RRL system, that alternate (nonproteasome) proteases might contribute to CFTR degradation, or, alternatively, that inhibitor effects might reflect a relative potency in blocking different proteasome peptidase activities. We therefore defined the effects of proteasome inhibitors on ChT-L, PGPH, and T-L activities of proteasomes in RRL under conditions used to carry out CFTR degradation. Our data indicate that each subunit can compensate for loss of other subunit activities, albeit to varying extents. Complete (>99.5%) inactivation of the  $\beta_5/X$  subunit decreased the rate of CFTR degradation by only 40%, whereas T-L activity was completely dispensable for degradation. Surprisingly, both  $\beta_1/Y$  and  $\beta_2/Z$  subunits were independently able to degrade CFTR at approximately 50% of the rate observed for fully functional proteasomes. The relative contribution of proteolytic activities to CFTR degradation resembled that reported for yeast proteasomes, ChT-L > PGPH  $\geq$  T-L, suggesting a conserved hierarchy of  $\beta$  subunit function that extends to mammalian proteasomes and to membrane-bound ERAD substrates.

## MATERIALS AND METHODS

**Materials.** *N*-Succinyl-Leu-Leu-Val-Tyr 7-amido-4-methylcoumarin (LLVY), *N*-tert-Boc-Leu-Arg 7-amido-4-methylcoumarin (LRR), Cbz-Leu-Leu-Leu-al (MG132), and leupeptin were purchased from Sigma (St. Louis, MO). Cbz-

Leu-Leu-Glu 7-amido-4-methylcoumarin (LLE) and *clasto*-lactacystin  $\beta$ -lactone were purchased from CalBiochem (San Diego, CA). GPFL-aldehyde was a generous gift of C. Cardozo. Nucleotides and DTT were purchased from Roche Molecular Biochemicals (Indianapolis, IN). EnHance was purchased from NEN Life Science Products (Boston, MA). Ready Safe scintillation fluid was purchased from Beckman (Fullerton, CA). Tran<sup>35</sup>S-label was purchased from ICN Pharmaceuticals (Irvine, CA).

**Cell-Free Transcription/Translation.** CFTR mRNA was transcribed in vitro at 40 °C for 1 h in reactions containing 0.4 mg/mL plasmid DNA [plasmid pSPCFTR (16)], 40 mM Tris (pH 7.5), 6.0 mM MgOAc<sub>2</sub>, 2 mM spermidine, 0.5 mM each of ATP, CTP, and UTP, 0.1 mM GTP, 0.5 mM GpppG (Amersham Pharmacia, Piscataway, NJ), 10 mM DTT, 0.2 mg/mL bovine calf tRNA, 0.75 unit/mL RNase inhibitor (Promega, Madison, WI), and 0.4 unit/mL SP6 RNA polymerase (New England Biolabs, Beverly, MA). Mock-transcription was identical except that no plasmid DNA was added. Transcript was either used immediately or stored frozen at –80 °C. Translation was performed at 24–25 °C for 2 h in a reaction containing 20% transcription mixture, 40% nuclease-treated rabbit reticulocyte lysate, 20% Emix, and a final concentration of 400  $\mu$ g/mL creatine kinase, 0.1 mg/mL tRNA, 0.2  $\mu$ L RNase inhibitor (Promega, Madison, WI), 10 mM Tris, pH 7.5, 100 mM KOAc, 2 mM MgCl<sub>2</sub>, and 2 mM DTT. Canine pancreas microsomal membranes, prepared as described elsewhere (28), were added at the start of translation. Emix contained 5 mM ATP, 5 mM GTP, 60 mM creatine phosphate, 0.2 mM each of 19 essential amino acids, except methionine, and 5  $\mu$ Ci/ $\mu$ L Tran<sup>35</sup>S-label; 50  $\mu$ M aurointricarboxylic acid was added 15 min after the start of translation to synchronize protein synthesis.

**Degradation Assay.** In vitro CFTR degradation was performed as reported previously (16) with the following modifications. ER membranes containing in vitro translated CFTR were collected by dilution into 2 volumes of Buffer A (0.1 M sucrose, 50 mM HEPES, pH 7.5, 0.1 M KCl, 5 mM MgCl<sub>2</sub>, and 1 mM DTT) and pelleted twice through 0.5 M sucrose, 50 mM HEPES (pH 7.5), 0.1 M KCl, 5 mM MgCl<sub>2</sub>, and 1 mM DTT at 180000g for 10 min. The resulting membrane pellet was washed once with Buffer A and vigorously resuspended in Buffer A (half of original translation volume). The degradation reaction contained 20% (by volume) microsomal membrane suspension, 68% (by volume) reticulocyte lysate [prepared as described (29)], 10 mM Tris (pH 7.5), 1 mM ATP, 5 mM MgCl<sub>2</sub>, 12 mM creatine phosphate, 3 mM DTT, and 80  $\mu$ g/mL creatine kinase. Degradation was carried out at 37 °C. Where indicated, RRL was replaced with water. ATP was depleted by substituting creatine kinase with hexokinase (20 units/mL) and deoxyglucose (20 mM). To quantitate the extent of degradation, samples were aliquoted into 20% trichloroacetic acid (TCA), incubated on ice for 30 min, and centrifuged at 16000g for 15 min. Supernatants (TCA-soluble counts) were counted in 10 volumes of Ready Safe scintillation fluid (Beckman, Fullerton, CA) in a Beckman LS6500 scintillation counter. Total <sup>35</sup>S in microsomes was determined by direct scintillation counting. For all degradation experiments (except those in Figure 1A), TCA-soluble counts were corrected for counts released in the absence of ATP because ATP-independent release from CFTR-containing membranes was equivalent to the release from mock-translated membranes. TCA-soluble

counts (CPM released) were expressed as a percentage of the total  $^{35}\text{S}$ -labeled CFTR present at  $T = 0$  using the formula:

$$\frac{[\text{CPM released} + \text{ATP}] - [\text{CPM released} - \text{ATP}]}{(\text{total incorporated } ^{35}\text{S} \times 0.78) - (\text{TCA-soluble CPM at } T = 0 \text{ min})}$$

This equation corrects for the fact that under the conditions used here, microsomes from mock-translations incorporated ~22% of the radioactivity found in microsomes containing translated CFTR. Although 90% of the radioactivity associated with “mock-translated” microsomes was TCA-precipitable, microsomes derived from mock-translations contained minimal radiolabeled protein when visualized by SDS-PAGE and autoradiography (data not shown). This background isotope incorporation is therefore unlikely due to translation of endogenous RNA, but rather appears to represent a reversible association of  $^{35}\text{S}$  species with components of ER microsomal membranes.

*Proteasome peptidase activities* were determined by measuring the rate of hydrolysis of fluorogenic peptide substrates according to Kanayama et al. (30). For inhibitor titration experiments, RRL concentration and the length of the incubation were adjusted so that the rate of hydrolysis remained linear over the time course of the reaction. ChT-L activity was measured at a 1:100 dilution of RRL in Buffer B (100 mM Tris, pH 8.0, 1 mM ATP, 1 mM DTT) using 100  $\mu\text{M}$  LLVY as substrate. T-L and PGPH activities were measured in RRL diluted 1:30 in Buffer B using 100  $\mu\text{M}$  LRR and 100  $\mu\text{M}$  LLE, respectively, as substrates. Reactions were carried out at 37 °C, and terminated by mixing each sample with an equal volume of 10% SDS, followed by 18 volumes of 100 mM Tris-HCl, pH 9.0. Free AMC was measured in opaque micro-titer plates using a BioRad FluoroMark plate reader (355 nm excitation/460 nm emission). Background fluorescence ( $T = 0$ ) was subtracted from each sample. Kinetic assays (Figure 2) were performed under the same conditions (and RRL concentration) used to measure CFTR degradation. Purified AMC was used to generate a standard curve to determine picomoles of AMC released in each experiment. Proteasome inhibition was expressed as the percent of control activity. Of note, inhibitor effects were linear over a wide range of RRL dilutions (data not shown). Resuspended proteasomes were prepared by diluting RRL 5-fold in 20 mM Tris-HCl, pH 7.5, 1 mM ATP, 1 mM  $\text{MgCl}_2$ , and 1 mM DTT, pelleting at 290000g for 2 h, and resuspending the resulting pellet in Buffer B at dilutions yielding activity equivalent to that found in RRL. Where indicated, assays were performed under conditions used to measure CFTR degradation (i.e., 40% RRL).

*Glycerol Gradient Centrifugation.* Reticulocyte lysate was diluted 1:10 in 20 mM Tris-HCl, pH 8.0, 1 mM ATP, and 1 mM DTT and layered over a 5–40% discontinuous glycerol gradient in 20 mM Tris-HCl, pH 8.0, 1 mM ATP, and 1 mM DTT. The gradient was centrifuged at 140000g for 2 h, and fractions were collected from top to bottom. Gradient fractions were diluted 1:1 with 2 $\times$  Buffer B containing either LLVY or LRR (100  $\mu\text{M}$  final concentration) and protease inhibitors as indicated. Samples were incubated at 37 °C, and 10  $\mu\text{L}$  samples were processed to determine AMC released as described above. The protein content of gradient fractions was determined by the method of Bradford (31).

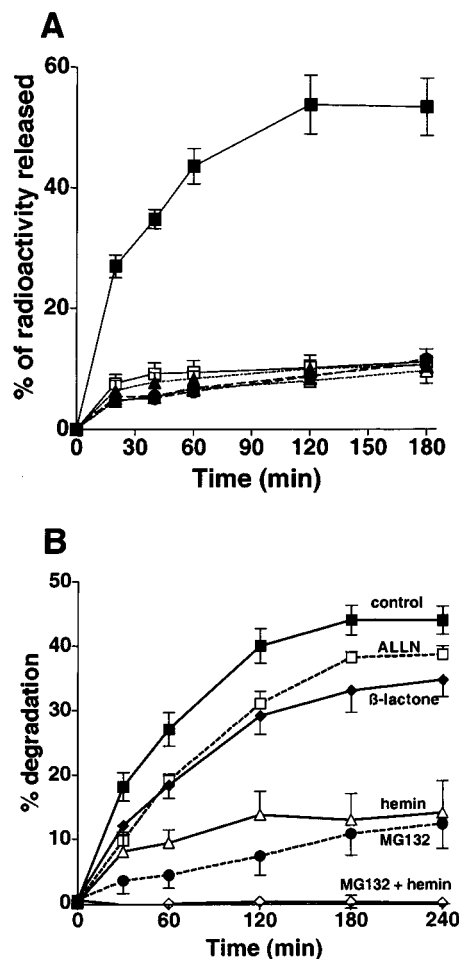


FIGURE 1: In vitro conversion of CFTR to TCA-soluble peptide fragments. (A) Translations were performed in the presence (closed symbols) or absence (open symbols) of CFTR message as described (Materials and Methods), and degradation was carried out in the presence (squares) or absence (triangles) of ATP, or of RRL (circles). “% of radioactivity released” refers to the fractional release of TCA-soluble counts relative to total incorporated TCA-insoluble counts at  $T = 0$  ( $\pm$ SEM). Fractional release from mock-translations is expressed as the percentage of TCA-insoluble counts incorporated during a CFTR translation. (B) ER microsomes containing radiolabeled CFTR were incubated in RRL in the absence (■) or presence of 100  $\mu\text{M}$   $\beta$ -lactone (◆), 100  $\mu\text{M}$  ALLN (□), 100  $\mu\text{M}$  MG132 (●), 40  $\mu\text{M}$  hemin (△), or 100  $\mu\text{M}$  MG132 + 40  $\mu\text{M}$  hemin (◇). Percent degradation was corrected to reflect release of TCA-soluble radioactivity derived solely from CFTR.

## RESULTS

*CFTR Degradation in RRL Is ATP-Dependent.* Previously we demonstrated that rabbit reticulocyte lysate (RRL) efficiently reconstitutes ubiquitination and degradation of newly synthesized CFTR in native ER microsomal membranes (16). Because CFTR is the only radiolabeled protein in this system, both the rate and the extent of its degradation can be directly determined by monitoring the production of TCA-soluble radiolabeled peptide fragments. As shown in Figure 1A, release of TCA-soluble radioactivity from CFTR-containing microsomal membranes exhibits two components: a large ATP-dependent component and a smaller ATP-independent component comprising 50–70% and ~10–15%, respectively, of microsome-associated  $^{35}\text{S}$  (16). Of note, the ATP-independent component was also released from microsomes derived from mock-translations (i.e., lacking  $^{35}\text{S}$ -labeled CFTR protein) both in the presence



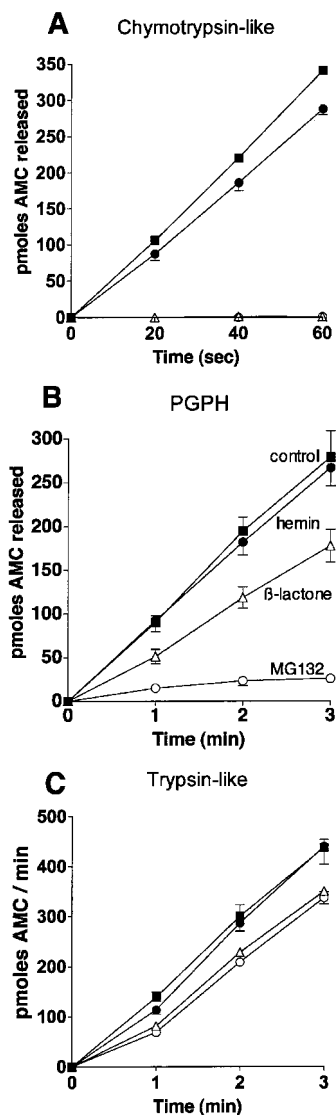


FIGURE 2: Activity of hemin,  $\beta$ -lactone, and MG132 on RRL proteasome activities. Fluorogenic peptide assays for ChT-L (A), PGPH (B), and T-L (C) activities were performed under conditions identical to those used to measure CFTR degradation. In each panel, cleavage of fluorogenic peptide substrate was performed in the absence of inhibitors (■), or in the presence of 40  $\mu$ M hemin (●), 100  $\mu$ M  $\beta$ -lactone (△), or 100  $\mu$ M MG132 (○). Values represent averages of at least three experiments  $\pm$  SEM.

and in the absence of RRL. Thus, this component is unrelated to CFTR degradation. Correcting for this background release revealed that ATP was absolutely required for conversion of CFTR into TCA-soluble fragments (Figure 1B).

**Effect of Proteasome Inhibitors on CFTR Degradation.** The strict ATP dependence of CFTR degradation in RRL is consistent with the energy requirements for ubiquitin conjugation and 26S proteasome function. Surprisingly, however, of the several proteasome inhibitors tested here and previously, only MG132 and hemin strongly inhibited the generation of TCA-soluble fragments [Figure 1B and (16)]. Two commonly used proteasome inhibitors, ALLN and clasto-lactacystin  $\beta$ -lactone ( $\beta$ -lactone), had significantly lesser effects on both the rate and the extent of degradation (Figure 1B). Several explanations could account for this observation. First, ALLN and  $\beta$ -lactone might be inactive in the RRL system. Second, the improved ability of MG132 to block CFTR degradation could be due to effects on an (alternate)

Table 1: Effect of Proteasome Inhibitors on RRL and Pelleted RRL Proteasomes

	inhibitor	IC <sub>50</sub> (SEM)		
		chymotrypsin-like	trypsin-like	PGPH
RRL	ALLN	4.6 $\mu$ M (0.3)	NA	36 $\mu$ M (2.0)
	MG132	14 nM (0.14)	NA	3.5 $\mu$ M (0.4)
	$\beta$ -lactone	4.4 $\mu$ M (0.5)	NA	112 $\mu$ M (11)
	GPFL	17 $\mu$ M (1.8)	NA	18 $\mu$ M (1.7)
290K pellet	ALLN	3.4 $\mu$ M (0.7)	60 $\mu$ M (7.4)	44 $\mu$ M (2.7)
	MG132	12 nM (0.63)	4.2 $\mu$ M (0.8)	3.1 $\mu$ M (0.4)
	$\beta$ -lactone	8.5 $\mu$ M (1.0)	22 $\mu$ M (4.1)	118 $\mu$ M (11)
	GPFL	18 $\mu$ M (1.0)	>500 $\mu$ M	18 $\mu$ M (0.5)
	leupeptin	>100 $\mu$ M	3.37 $\mu$ M (0.4)	>100

ATP-dependent nonproteasomal protease as suggested previously (24). Third, the different effects of proteasome inhibitors could reflect their relative efficacy at inhibiting different proteasome  $\beta$  subunits. We therefore determined, first, whether these inhibitors were active in RRL by monitoring proteasome ChT-L, T-L, and PGPH activities using site-specific fluorogenic peptide substrates: LLVY, LRR, and LLE. Cleavage of these substrates by proteasome  $\beta_5$ /X,  $\beta_1$ /Y, and  $\beta_2$ /Z subunits, respectively, releases AMC and allows direct measurement of individual subunit proteolytic activity (32, 33). Because RRL does not contain immunoproteasomes (34), our analysis was limited to standard proteasome proteolytic activities.

Initial peptidase assays were performed under experimental conditions identical to those used for CFTR degradation and demonstrated that both  $\beta$ -lactone and MG132 were highly active in RRL, inhibiting >99% of ChT-L activity (Figure 2A).  $\beta$ -Lactone was significantly less effective against PGPH and T-L activities (Figure 2B,C), consistent with previous studies (33, 35); while the proteasome ATPase inhibitor hemin had minimal effects on peptidase activities (Figure 2A–C). ALLN,  $\beta$ -lactone and MG132 each effectively blocked ChT-L activity with an IC<sub>50</sub> of <10  $\mu$ M (Figure 3 and Table 1), and their relative potency, MG132  $\gg$   $\beta$ -lactone > ALLN, was similar to that described for purified proteasomes (33, 36).  $\beta$ -Lactone and ALLN were much less effective than MG132 at blocking PGPH activity (IC<sub>50</sub> > 100  $\mu$ M, ~40  $\mu$ M, and 5  $\mu$ M, respectively), again consistent with previous studies. Thus, it is unlikely that the different effects of proteasome inhibitors on CFTR degradation were due to inhibitor inactivation by components present in RRL. Interestingly, none of the proteasome inhibitors tested effectively blocked RRL T-L activity (Figure 3C), raising the possibility that other proteolytic activities of RRL might contribute to CFTR degradation. Leupeptin, which inhibits the T-L activity of purified proteasomes (37), also inhibited only ~60% of RRL T-L activity (Figure 4A), and this effect was not additive to that of MG132. Residual T-L proteolytic activity, however, was significantly inhibited both by EGTA and by the aminopeptidase inhibitor bestatin. This effect of EGTA was reversed by zinc (Figure 4A, inset), suggesting the presence of one or more metallo-exopeptidases in RRL (38).

To further define protease activities involved in CFTR degradation, RRL was separated by glycerol gradient centrifugation. ChT-L activity migrated at the predicted size of the 26S proteasome and was completely abolished by MG132 (Figure 4B). Similar results were obtained for PGPH activity (data not shown). T-L activity was present as two heterogeneous peaks (Figure 4C). The higher molecular weight

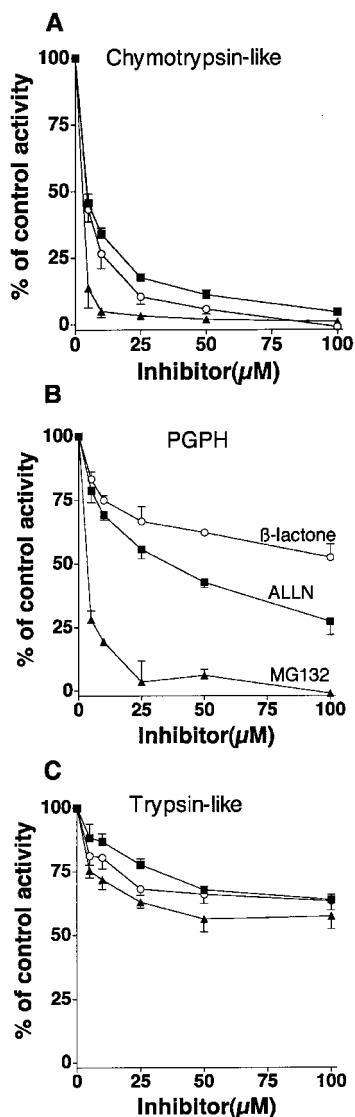


FIGURE 3: Dose dependence of proteasome inhibitors in RRL. ChT-L (A), PGPH (B), and T-L (C) activities were measured using the fluorogenic peptides LLVY, LLE, and LRR, respectively, as described under Materials and Methods. Reactions were carried out in the presence of varying concentrations of ALLN (■),  $\beta$ -lactone (○), and MG132 (▲) as indicated, and peptide hydrolysis was expressed as % of control activity observed in the absence of inhibitors. Values represent average of at least three experiments  $\pm$  SEM.

protease comigrated with ChT-L activity and was sensitive to MG132. The lower molecular weight protease was unaffected by MG132, inhibited by EGTA, and reversed by zinc. Thus, the refractory T-L activity(ies) in RRL is (are) clearly not due to intrinsic resistance of the proteasome but rather to additional RRL protease(s) (39). For unclear reasons, separation of 26S proteasomes on glycerol gradients appeared to increase the apparent T-L activity, as reflected in the higher ratio of MG132 sensitive to resistant T-L activity in gradient fractions (80%) compared to unfractionated RRL (45–55%; see Figures 3C and 4A).

To determine whether this proteolytic activity was involved in CFTR degradation, we examined whether EGTA and/or bestatin influenced the generation of CFTR-derived TCA-soluble fragments. Neither compound alone, together, or in combination with various proteasome inhibitors had a significant effect on either the rate or the extent of CFTR

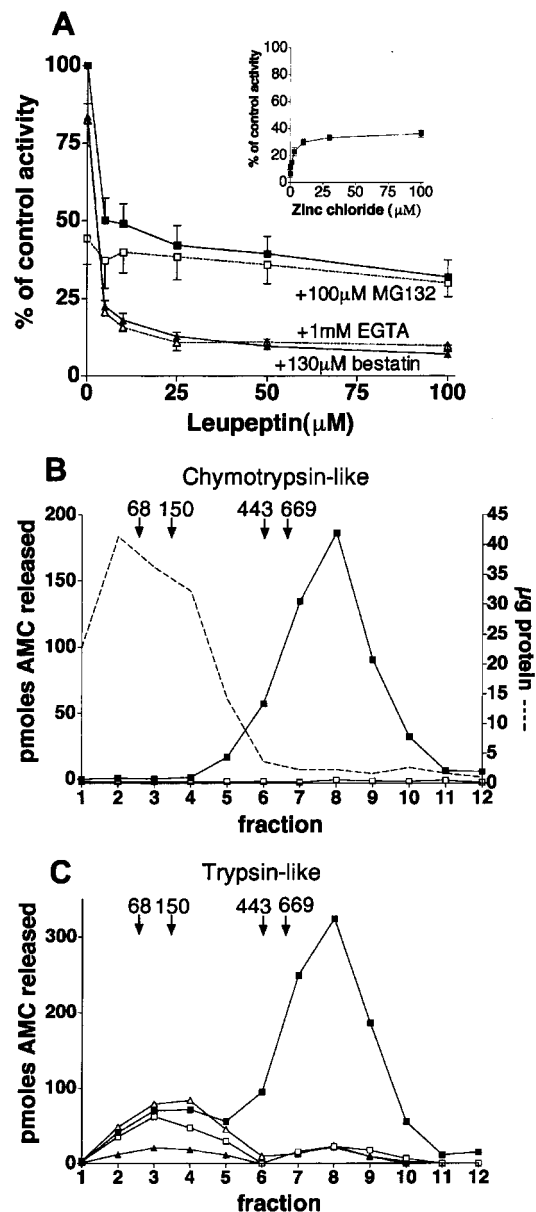


FIGURE 4: Identification of a nonproteasome RRL T-L peptidase activity. (A) T-L activity of dilute RRL was measured in the presence of leupeptin, either alone (■) or together with 100  $\mu$ M MG132 (□), 1 mM EGTA (△), or 130  $\mu$ M bestatin (▲). Inset: T-L activity in the presence of 100  $\mu$ M leupeptin, 1 mM EGTA, and increasing concentrations of  $ZnCl_2$ . (B) RRL was separated by glycerol gradient centrifugation, and individual fractions were assayed for total protein (dashed line) and ChT-L activity (solid line) in the absence (■) or presence (□) of 100  $\mu$ M MG132. Arrows at top indicate positions of molecular weight standards in the gradient. (C) T-L activity of gradient fractions measured in the absence (■), or in the presence of 100  $\mu$ M MG132 (□), 100  $\mu$ M MG132 + 1 mM EGTA (▲), or 100  $\mu$ M MG132 + 1 mM EGTA + 100  $\mu$ M  $ZnCl_2$  (△). The activities in panels B and C indicate picomoles of AMC released from the fluorogenic substrates per minute, and are representative of at least three experiments.

degradation (Figure 5). Similar results were obtained for the serine protease inhibitor phenylmethylsulfonyl fluoride (Figure 5A and data not shown) as well as a wide variety of other nonproteasome protease inhibitors (16). Thus, it is unlikely that the refractory T-L activity or other RRL proteases are responsible for the generation of CFTR-derived TCA-soluble fragments observed in the presence of proteasome inhibitors. These results, together with the strict ATP

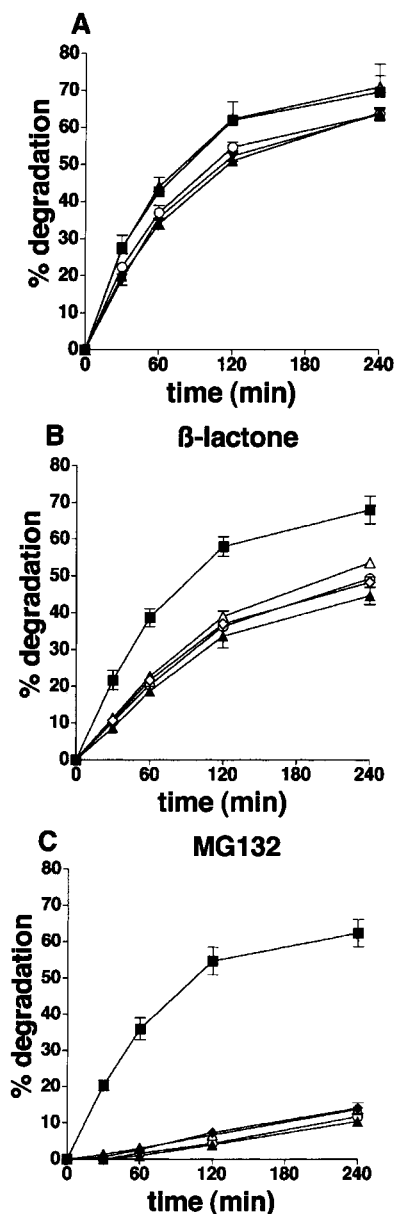


FIGURE 5: Additive effects of proteasome and nonproteasome inhibitors. (A) CFTR degradation was carried out in the absence of inhibitors (■) or in the presence of 1 mM EGTA (△), 130 μM bestatin (▲), 500 μM PMSF (○), or the combination of EGTA, bestatin, and PMSF (▼). (B) Same as panel A except that EGTA, bestatin, and PMSF were individually evaluated in combination with 100 μM β-lactone. (C) Same as panel A except that EGTA, bestatin, and PMSF were individually evaluated in combination with 100 μM MG132. Degradation was also carried out with β-lactone (◇) or MG132 (◆) alone in panels B and C, respectively. Data show average of three consecutive experiments ±SEM.

dependence and hemin sensitivity, provide strong evidence that the 26S proteasome plays a central role in ER-associated CFTR degradation.

**Sensitivity of Pelleted RRL Proteasomes to Proteasome Inhibitors.** Considering the results of Figure 4, we next determined the ability of inhibitors to block β subunit function(s) using proteasomes separated from RRL by ultracentrifugation. ChT-L and PGPH activities in pelleted proteasomes exhibited similar sensitivities to ALLN, β-lactone, and MG132 as those observed for unfractionated RRL (Figure 6 and Table 1), supporting our hypothesis that these agents were not affected by other RRL components. More-

over, both leupeptin and MG132 now strongly inhibited the T-L activity of pelleted proteasomes ( $IC_{50} = 3.4$  and  $4.2$  μM, respectively). Of the five different agents tested, only MG132 effectively inhibited all three active β subunits (by >93%). ALLN and β-lactone were potent inhibitors of ChT-L activity ( $IC_{50} \sim 3$  and  $8$  μM, respectively) but were relatively weak inhibitors of T-L and PGPH activity (Figure 6B,C and Table 1). The peptide aldehyde cbz-GPFL-CHO, which also inhibits the immunoproteasome (40), was highly selective for the ChT-L and PGPH activities (Figure 6D). The effects of inhibitors on proteolytic activities of pelleted RRL proteasomes were very similar to those previously reported for purified mammalian proteasomes (32, 33).

**All Three Proteasome β Subunits Can Contribute to ATP-Dependent CFTR Degradation.** Based on the findings that hydrolysis of fluorogenic peptide substrates accurately reflects individual β subunit proteolytic activities (4, 5, 10, 13, 41), we determined the relative ability of different β subunits to carry out CFTR degradation by testing various combinations of inhibitors. For these experiments, degradation was carried out as in Figure 1B, and inhibition was expressed as the fractional decrease in the initial rate with which CFTR was converted into TCA-soluble fragments. As shown in Figure 7, isolated inhibition of T-L activity had no effect on CFTR degradation. This is consistent with genetic studies in yeast demonstrating that T-L activity is not essential for proteasome function (5, 12). Inhibition of ChT-L activity (by >99%) with β-lactone, ALLN, or cbz-GPFL-CHO decreased the rate of CFTR degradation by only ~40%. Interestingly, cbz-GPFL-CHO was no more effective in blocking CFTR degradation than ALLN or β-lactone despite its significantly greater inhibition of PGPH activity (~96% inhibition). This suggested that the T-L activity alone might be sufficient to facilitate CFTR degradation, albeit at a reduced rate. Consistent with this hypothesis, the rate of CFTR degradation was further reduced when leupeptin was added to cbz-GPFL-CHO (a 50% decrease from cbz-GPFL-CHO alone). Results of MG132 and the combination of three separate proteasome β subunits (cbz-GPFL-CHO, leupeptin, and β-lactone) demonstrated that the cumulative inhibition of all three proteasome β subunits was closely correlated to the rate of CFTR degradation (89% decrease for MG132 and 94% decrease for the combined inhibitors). Complete inhibition of degradation was observed only when active site inhibitors (e.g., MG132) were combined with the proteasome ATPase inhibitor, hemin.

## DISCUSSION

In this study, we have used active site inhibitors and a reconstituted cell-free system to determine the relative ability of proteasome β subunits to carry out ER-associate degradation of CFTR, a polytopic integral membrane protein. This system enabled us to measure both the rate of substrate degradation as well as the β subunit activity under experimental conditions that mimic the intracellular environment at the ER membrane. Our results demonstrate both a hierarchy and a functional redundancy of proteasome β subunits. Inhibitors that primarily target the β<sub>5</sub> subunit (ChT-L activity) such as β-lactone and ALLN decreased the rate of CFTR degradation by approximately 40%, while inactivation of the β<sub>2</sub> subunit (T-L activity) had no effect. Interestingly, reducing the rate of CFTR degradation by β<sub>5</sub> inhibition did not translate into a corresponding reduction

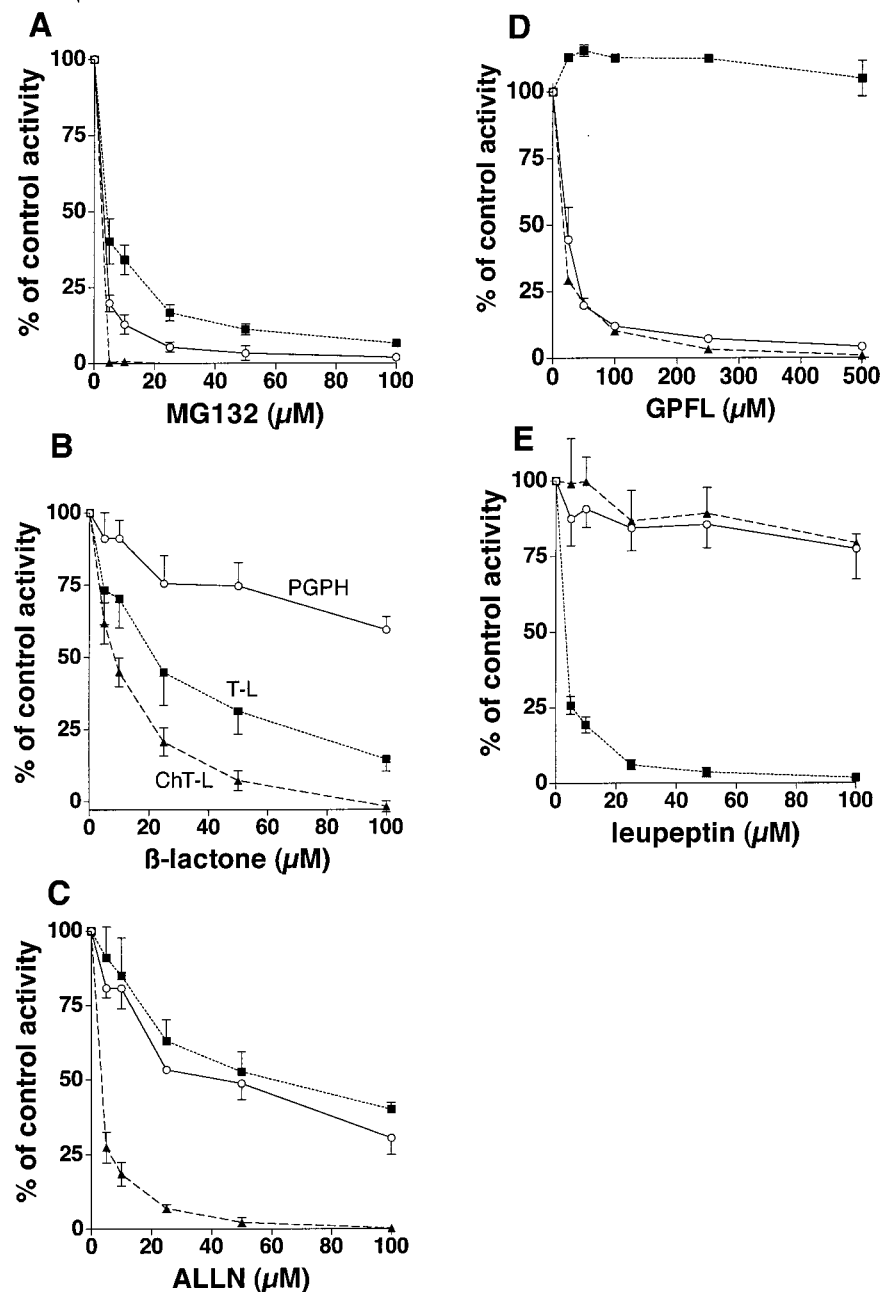


FIGURE 6: Inhibition of protease activities in pelleted RRL proteasomes. Proteasome complexes were collected from RRL by centrifugation at 290000g for 2 h, and the pellet was resuspended and assayed for T-L (■), PGPH (○), or ChT-L (▲) activity in the presence of increasing concentrations of (A) MG132, (B)  $\beta$ -lactone, (C) ALLN, (D) cbz-GPFL-CHO, or (E) leupeptin. Assay conditions were the same as in Figure 3.

in the extent of degradation. Of the individual agents tested here and previously (16), MG132 was most active, reducing the rate and extent of CFTR conversion to TCA-soluble fragments by ~90% and 75%, respectively. In this regard, two features distinguish MG132 from  $\beta$ -lactone and ALLN: (i) its extremely high affinity for the  $\beta_5$  subunit and (ii) its ability to simultaneously inhibit all three proteasome peptidase activities. cbz-GPFL-CHO combined with  $\beta$ -lactone decreased ChT-L and PGPH activities to a similar extent as MG132 but had a lesser effect on the rate of CFTR degradation. Addition of leupeptin, which had no independent effect on degradation, to cbz-GPFL-CHO and  $\beta$ -lactone resulted in the cumulative inhibition of all three  $\beta$  subunits and reproduced the effect observed for MG132. Taken together, these data indicate that  $\beta_1$  and  $\beta_2$  subunits, although

not required for degradation, are able to independently degrade CFTR at nearly half the rate of that observed for fully active proteasomes. Moreover, >90% inhibition of CFTR degradation required that all three proteasome activities be significantly inhibited (by >93%) and that ChT-L activity be very strongly inhibited. Even under these conditions, however, a small amount of TCA-soluble degradation products continued to be generated but only in the presence of proteasome ATPase activity.

Given the strict ATP dependence, the lack of involvement of cysteine, serine, and metalloproteinases [Figure 5 and (16)], and the cumulative effects of multiple proteasome active site and ATPase inhibitors, the simplest explanation of our findings is that each proteasome  $\beta$  subunit is capable of independently contributing to CFTR degradation. More-



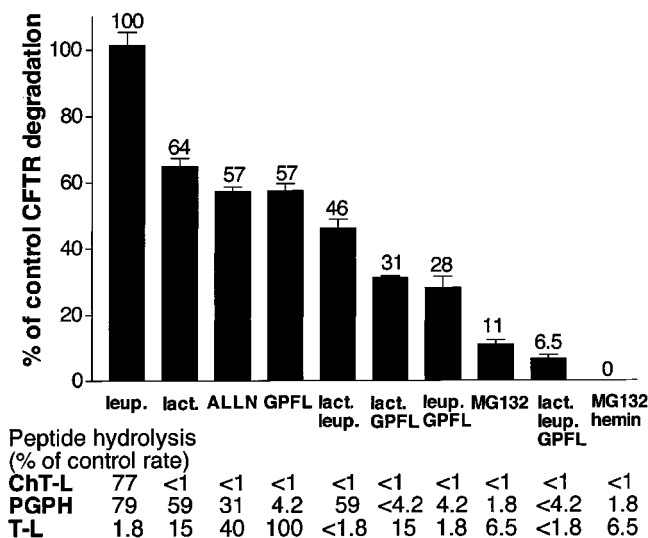


FIGURE 7: Relative contribution of proteasome  $\beta$  subunits to CFTR degradation. CFTR degradation was carried out as in Figures 1 and 5. The initial rate (0–30 min) of CFTR conversion to TCA-soluble fragments is expressed as a percentage of degradation under control conditions. Assays were performed in the presence of 100  $\mu$ M leupeptin (leup.), 100  $\mu$ M  $\beta$ -lactone (lact.), 100  $\mu$ M ALLN (ALLN), 500  $\mu$ M cbz-GPFL-CHO (GPFL), 100  $\mu$ M MG132 (MG132), and 40  $\mu$ M hemin (hemin), either alone or in the combinations indicated. Percent residual activity is indicated above each column. Listed below each column are the rates of fluorogenic peptide hydrolysis for each  $\beta$ -subunit at the same inhibitor concentration (expressed as a percent of the control rate).

over, even minor residual activity of a single  $\beta$  subunit appears sufficient to generate TCA-soluble peptide fragments, although at a greatly reduced rate. Consistent with these results, purified yeast 20S proteasomes that lack functional  $\beta_5$ /Pre2/Doa3 subunits were able to degrade enolase into peptide fragments of similar length as those generated by wild-type proteasomes (13). This is presumably because  $\beta_1$  and  $\beta_2$  subunits, in addition to their PGPH and T-L activities, can also cleave complex protein substrates at sites that do not contain charged residues (8). This overlapping specificity, however, does not appear to apply to fluorogenic peptide substrates which have been shown by genetic studies to provide a relatively accurate measure of individual  $\beta$  subunit activities (8, 13). Similarly, cells treated with NIP-Leu-Leu-Leu-vinyl sulfone (NLVS) contain proteasomes with covalently inactivated  $\beta_5$  and  $\beta_2$  subunits. Yet these cells still exhibit residual proteasome activity that is required for growth, antigen presentation, and degradation of polyubiquitinated proteins (14). Our results now provide additional and quantitative evidence for a redundancy in mammalian  $\beta$  subunit function and extend this property to native ER substrates.

In yeast, the  $\beta_5$ /Pre2/Doa3 subunit (ChT-L activity) is required for cell growth, protection from stress, and normal degradation of ubiquitinated proteins (4). In contrast, genetic inactivation of  $\beta_2$ /Pup1 or  $\beta_1$ /Pre3 subunits resulted in mild or no phenotypic changes (4, 5, 10, 12). Our results are consistent with these findings and suggest that mechanisms governing proteasome-mediated protein turnover are remarkably conserved in yeast and in the mammalian ERAD pathway. Interestingly, inactivation of the yeast  $\beta_5$ /Pre2/Doa3 subunit resulted in a 6-fold decrease in degradation of MAT  $\alpha_2$ , even when proteasome assembly was restored by coexpression of the  $\beta_5$ /Pre2/Doa3 leader peptide (4). In RRL,

however, >99.5% inhibition of the mammalian  $\beta_5$  subunit decreased ATP-dependent CFTR degradation by less than 2-fold and had almost no effect on the extent of degradation. While we cannot rule out whether these results reflect experimental conditions or subtle differences between yeast and mammalian proteasomes, they raise the possibility that endogenous protein substrates might exhibit different relative susceptibilities to degradation by different proteasome  $\beta$  subunits. Such a possibility would be consistent with the finding that degradation of enolase by  $\beta_5$ -deficient yeast proteasomes generated a distinctly different set of peptide fragments than wild-type proteasomes (8). This may also potentially explain why ALLN and lactacystin blocked degradation of mutant  $\alpha_1$ -antitrypsin and MHC Class 1 heavy chains in RRL (42, 43) and yet had relatively little effect on CFTR.

An important question raised by this and other studies (24) is whether nonproteasome proteases such as tricorn protease, tripeptidyl peptidase II (TPPII), or others might also participate in CFTR degradation. In this regard, overexpression of TPPII, a multimeric serine protease, reproduced the adaptation of EL-4 cells to proteasome inhibition by NLVS (44, 45), suggesting a complementary function for these two proteolytic systems. While TPPII is present at high levels in rabbit erythrocytes (46), two lines of evidence indicate that it is not involved in generating CFTR-derived TCA-soluble fragments. First, unlike ALLN, 100  $\mu$ M lactacystin inhibits ~95% of TPPII activity (47). Yet ALLN and  $\beta$ -lactone had nearly identical effects on CFTR degradation in RRL. Second, PMSF, an irreversible inhibitor of TPPII, had no effect on CFTR degradation either alone or in combination with  $\beta$ -lactone, ALLN, or MG132 [Figure 5, data not shown and (16)]. We also identified a nonproteasome T-L activity in RRL that was refractory to standard proteasome inhibitors. Based on its size and sensitivity to bestatin and EGTA, this proteolytic activity likely consists of one or more aminopeptidases present in RRL (38). Importantly, we have been unable to implicate this or any other RRL proteolytic activities in CFTR degradation. While it remains possible that proteases other than the proteasome may participate in either the initial or the final stages of the degradation pathway, our data suggest that the proteasome itself is the major protease involved in the conversion of CFTR into TCA-soluble peptide fragments.

Previous studies have shown that in RRL, MG132 causes a transient accumulation of CFTR in a high molecular weight ubiquitinated complex that gradually disappears when examined by SDS-PAGE (16). However, as shown in the current study, MG132 effectively blocks the production of CFTR-derived TCA-soluble fragments. This apparent discrepancy could be explained if, by targeting all three active  $\beta$  subunits, MG132 resulted in less frequent cleavage of substrate within the catalytic core of the 20S particle, thus generating larger protein fragments at the expense of small TCA-soluble peptides. Such a mechanism would predict that MG132 (more so than ALLN or  $\beta$ -lactone) would cause release of larger peptide fragments into the cytosol, a finding confirmed by additional studies in our laboratory (J.O. and W.R.S., manuscript in preparation).

Consistent with our observations, proteasome inhibitors slow, but do not fully inhibit CFTR degradation *in vivo* (24, 25). We propose that the slow degradation observed in cells is likely due to residual activity of intact  $\beta_1$  and/or  $\beta_2$



subunits. It should also be noted that unlike ALLN and lactacystin, MG132 has the unique effect of preventing CFTR maturation in cells (24). Although this could result from inhibition of a nonproteasomal protease(s) as previously suggested (24), our data raise the additional possibility that by blocking all three proteasome  $\beta$  subunits, MG132 should have greater effects on protein degradation in general, which in turn could influence other cellular processes involved in CFTR maturation. This prediction is supported by the more vigorous cellular stress response observed for MG132 when compared to lactacystin or ALLN (48). Taken together, our studies highlight an important relationship between proteasome inhibitors and the physiologic degradation of endogenous protein substrates. The net effect of a given inhibitor results from the cumulative inhibition of multiple  $\beta$  subunits within the 26S proteasome complex.

## ACKNOWLEDGMENT

We thank Dr. C. Cardozo for generously providing GPFL-aldehyde and Dr. Linda Musil, Dr. Dennis Koop, and members of the Skach lab for their helpful comments.

## REFERENCES

1. Brodsky, J., and McCracken, A. (1997) *Trends Cell Biol.* 7, 151–155.
2. Kopito, R. (1997) *Cell* 88, 427–430.
3. Hershko, A., and Ciechanover, A. (1998) *Annu. Rev. Biochem.* 67, 425–479.
4. Chen, P., and Hochstrasser, M. (1996) *Cell* 86, 961–972.
5. Heinemeyer, W., Fischer, M., Krimmer, T., Stachon, U., and Wolf, D. (1997) *J. Biol. Chem.* 272, 25200–25209.
6. Chen, H., and Hochstrasser, M. (1995) *EMBO J.* 14, 2620–2630.
7. Groll, M., Ditzel, L., Lowe, J., Stock, D., Bochtler, M., Bartunik, H., and Huber, R. (1997) *Nature* 386, 463–471.
8. Dick, T., Nussbaum, A., Deeg, M., Heinemeyer, W., Groll, M., Schirle, M., Keilholz, W., Stevanovic, S., Wolf, D., Huber, R., Rammensee, H., and Schild, H. (1998) *J. Biol. Chem.* 273, 25637–25646.
9. Jäger, S., Groll, M., Huber, R., Wolf, D., and Heinemeyer, W. (1999) *J. Mol. Biol.* 291, 997–1013.
10. Arendt, C., and Hochstrasser, M. (1999) *EMBO J.* 18, 3575–3585.
11. Gueckel, R., Enenkel, C., Wolf, D., and Hilt, W. (1998) *J. Biol. Chem.* 273, 19443–19452.
12. Arendt, C., and Hochstrasser, M. (1997) *Proc. Natl. Acad. Sci. U.S.A.* 94, 7156–7161.
13. Nussbaum, A., Dick, T., Keilholz, W., Schirle, M., Stevanovic, S., Dietz, K., Heinemeyer, W., Groll, M., Wolf, D., Huber, R., Rammensee, H., and Schild, H. (1998) *Proc. Natl. Acad. Sci. U.S.A.* 95, 12504–12509.
14. Princiotta, M., Schubert, U., Chen, W., Bennink, J., Myung, J., Crews, C., and Yewdell, J. (2001) *Proc. Natl. Acad. Sci. U.S.A.* 98, 513–518.
15. Plemper, R., and Wolf, D. (1999) *Trends Biol. Sci.* 24, 266–270.
16. Xiong, X., Chong, E., and Skach, W. (1999) *J. Biol. Chem.* 274, 2616–2624.
17. Plemper, R., Egner, R., Kuchler, K., and Wolf, D. (1998) *J. Biol. Chem.* 273, 32848–32856.
18. Bebok, Z., Mazzochi, C., King, S., Hong, J., and Sorscher, E. (1998) *J. Biol. Chem.* 273, 29873–29878.
19. Wiertz, E., Tortorella, D., Bogoyo, M., Yu, J., Mothes, W., Jones, T., Rapoport, T., and Ploegh, H. (1996) *Nature* 384, 432–438.
20. Wiertz, E., Jones, T., Sun, L., Bogoyo, M., Geuze, H., and Ploegh, H. (1996) *Cell* 84, 769–779.
21. Yu, H., Kaung, S., Kobayashi, S., and Kopito, R. (1997) *J. Biol. Chem.* 272, 20800–20804.
22. McCracken, A., and Brodsky, J. (1996) *J. Cell Biol.* 132, 291–298.
23. Riordan, J. R., Rommens, J. M., Kerem, B.-S., Alon, N., Rozmahel, R., Grzelczak, Z., Zielenski, J., Lok, S., Collins, F. S., and Tsui, L.-C. (1989) *Science* 245, 1066–1072.
24. Jensen, T., Loo, M., Pind, S., Williams, D., Goldberg, A., and Riordan, J. (1995) *Cell* 83, 129–136.
25. Ward, C., Omura, C., and Kopito, R. (1995) *Cell* 83, 121–128.
26. Hoffman, L., and Rechsteiner, M. (1996) *J. Biol. Chem.* 271, 32538–32545.
27. Lee, D., and Goldberg, A. (1998) *Trends Cell Biol.* 8, 397–403.
28. Walter, P., and Blobel, G. (1983) *Methods in Enzymology* (Fleischer, S., and Fleischer, B., Eds.) pp 84–93, Academic Press, Inc., New York.
29. Oberdorf, J., and Skach, W. (2001) *Cystic Fibrosis: Methods and Protocols* (Skach, W., Ed.) Humana Press, Totowa, NJ.
30. Kanayama, H., Tamura, T., Ugai, S., Kagawa, S., Tanahashi, N., Yoshimura, S., Tanaka, K., and Ichihara, A. (1992) *Eur. J. Biochem.* 206, 567–578.
31. Bradford, M. (1976) *Anal. Biochem.* 72, 248–254.
32. Bogoyo, M., Shin, S., McMaster, J., and Ploegh, H. (1998) *Chem. Biol.* 5, 307–320.
33. Bogoyo, M., McMaster, J., Gaczynska, M., Tortorella, D., Goldberg, A., and Ploegh, H. (1997) *Proc. Natl. Acad. Sci. U.S.A.* 94, 6629–6634.
34. Ustrell, V., Realini, C., Pratt, G., and Rechsteiner, M. (1995) *FEBS Lett.* 376, 155–158.
35. Fenteany, G., Standaert, R., Lane, W., Choi, S., Corey, E., and Schreiber, S. (1995) *Science* 268, 726–731.
36. Rock, K., Gramm, C., Rothstein, L., Clark, K., Stein, R., Dick, L., Hwang, D., and Goldberg, A. (1994) *Cell* 78, 761–771.
37. Savory, P., and Rivett, J. (1993) *Biochem. J.* 289, 45–48.
38. Melloni, E., Salamino, F., Sparatore, B., Michetti, M., Morelli, A., Benatti, U., De Flora, A., and Pontremoli, S. (1981) *Biochim. Biophys. Acta* 675, 110–116.
39. Hough, R., Pratt, G., and Rechsteiner, M. (1987) *J. Biol. Chem.* 262, 8303–8313.
40. Vinitzky, A., Cardozo, C., Sepp-Lorenzino, L., Michaud, C., and Orlowski, M. (1994) *J. Biol. Chem.* 269, 29860–29866.
41. Arispe, N., Rojas, E., Hartman, J., Sorscher, E., and Pollard, H. (1992) *Proc. Natl. Acad. Sci. U.S.A.* 89, 1539–1543.
42. Wilson, C., Farmery, M., and Bulleid, N. (2000) *J. Biol. Chem.* 275, 21224–21232.
43. Qu, D., Teckman, J., Omura, S., and Perlmutter, D. (1996) *J. Biol. Chem.* 271, 22971–22975.
44. Glas, R., Bogoyo, M., McMaster, J., Gaczynska, M., and Ploegh, H. (1998) *Nature* 392, 618–622.
45. Wang, E., Kessler, B., Borodovsky, A., Cravatt, B., Bogoyo, M., Ploegh, H., and Glas, R. (2000) *Proc. Natl. Acad. Sci. U.S.A.* 97, 9990–9995.
46. Balow, R.-M., and Eriksson, I. (1987) *Biochem. J.* 241, 75–80.
47. Geir, E., Pfeifer, G., Wilm, M., Lucchiari-Hartz, M., Baumeister, W., Eichmann, K., and Niedermann, G. (1999) *Science* 283, 978–981.
48. Bush, K., Goldberg, A., and Nigam, S. (1997) *J. Biol. Chem.* 272, 9086–9092.

BI011322Y